Modelling mid-Holocene tropical climate and ENSO variability: towards constraining predictions of future change with palaeo-data

Josephine Brown · Matthew Collins · Alexander W. Tudhope · Thomas Toniazzo

Abstract Palaeoclimate simulations provide an opportunity for climate model evaluation as well as having a potential role in assigning relative likelihood to different ensemble members in probabilistic climate change prediction, supplementing constraints provided by the instrumental record. Here we take some initial steps towards such an approach by performing ensemble experiments with the Hadley Centre HadCM3 model under pre-industrial and mid-Holocene (6,000 years before present) forcing conditions. We examine the changes in both mean tropical climate and El Niño-Southern Oscillation (ENSO) variability, as palaeoclimate records suggest that ENSO amplitude was reduced in the mid-Holocene. Experiments are performed with perturbations to physical parameters in the atmosphere–surface component of the model, and with different implementations of heat and freshwater flux adjustments. Heat flux adjustments are required to stabilise model versions in which perturbations cause a net radiative imbalance. While we find broad agreement between different model versions in terms of changes in mean climate in the mid-Holocene, a detailed and quantitative comparison with the geographically-sparse palaeo-record is limited by systematic model biases. In the simulations without seasonally-varying flux adjustments there are modest reductions in ENSO amplitude of the order of 10–15%, lower than the range of reductions inferred from coral proxy records. We examine the mechanisms for these changes, and discuss the implications for the design of future ensemble experiments to formally quantify uncertainty in climate change predictions using palaeoclimate simulations.

J. Brown (✉)
School of Geography and Environmental Science,
Monash University, Clayton, VIC 3800, Australia
e-mail: josephine.brown@arts.monash.edu.au

J. Brown
Department of Meteorology,
University of Reading, Reading, UK

M. Collins · T. Toniazzo
Hadley Centre, Met Office, Exeter, UK

A. W. Tudhope
School of Geosciences,
University of Edinburgh,
Edinburgh, UK

1 Introduction

Predictions of future changes in climate are uncertain because of unknown future concentrations of greenhouse gases and other forcing agents, because of unpredictable natural fluctuations in the climate system and because of imperfections in the models we use to make predictions. Recent studies have sought to quantify the latter sources of uncertainty by performing ensemble experiments with climate models (under idealised equilibrium forcing) and constraining predictions of global mean change by assigning relative weights to ensemble members according to their ability to simulate present day conditions (e.g. Murphy et al. 2004; Piani et al. 2005; Tebaldi et al. 2005; Knutti et al. 2006). Past climates, while not providing a direct analogue of future changes, present a further potential constraint on model sensitivity and provide the focus for this study.

A specific example of uncertain model predictions is the response of El Niño-Southern Oscillation (ENSO) to future climate change. Different models project a wide range of responses from weakened to strengthened ENSO (e.g. van Oldenborgh et al. 2005; Guilyardi et al. 2006; Merryfield 2006). Changes in the mean state of the tropics are also uncertain, with models simulating responses ranging from ''El Niño-like'' to ''La Niña-like'' changes in tropical Pacific zonal SST gradients (e.g. Collins et al. 2005; Merryfield 2006). While the ability of coupled atmosphere–ocean models to simulate ENSO has improved dramatically in recent years (e.g. Latif et al. 2001; AchutaRao and Sperber 2002, 2006), such models may not yet accurately represent all the complex interactions between processes necessary to simulate the response of ENSO to changes in mean climate (e.g. Fedorov and Philander 2000; Cane 2005). Given the importance of predicting future changes in ENSO, and in the absence of a perfect model, it is necessary to quantify the uncertainty associated with predictions from current generation models.

In this study, we explore uncertainty in model ENSO sensitivity by testing the ability of models to simulate palaeoclimate conditions, when proxy records imply that the mean state and interannual variability in the tropics were substantially different from present. Palaeoclimate simulations provide an independent test of model sensitivity in response to external forcing and changes in the mean state, which are outside the range of conditions observed in the instrumental period. The mid-Holocene (6,000 years before present, 6 ka) is an appropriate target for such a study, as boundary conditions including atmospheric composition and orbital configuration are well known. In addition, palaeoclimate records of changes in both mean state and interannual variability in the tropics are available for comparison with the model simulations.

During the mid-Holocene, the change in the timing of perihelion from boreal winter to boreal summer resulted in an increased northern hemisphere (NH) seasonal cycle, while reducing the strength of southern hemisphere (SH) seasonality. As modern ENSO is observed to be strongly phase-locked to the seasonal cycle (e.g. Tziperman et al. 1997; Wang and Picaut 2004), it might be expected that such a change in the seasonal cycle would alter the behaviour of ENSO. The global mean climate in the mid-Holocene was broadly similar to the present as the NH continental ice sheets of the Last Glacial period had largely melted by this time and the atmospheric carbon dioxide concentration was close to pre-industrial values (e.g. Indermuhle et al. 1999). The response of ENSO to orbital changes in seasonality, while not being analogous to the case of anthropogenic global warming, does present a verifiable test of the sensitivity of ENSO in coupled climate

models to climate forcing. The challenge is to make a quantitative comparison between the model and palaeo-data in order to assign a relative weight to each member of a large ensemble. Recognising that this is a considerable and long-term research undertaking, we present a preliminary attempt at generating such an ensemble in this study.

The mean state of Holocene tropical Pacific SSTs and salinity has been reconstructed from palaeoclimate records including oxygen isotope ratios and Mg/Ca ratios in planktonic foraminifera (e.g. Koutavas et al. 2002; Stott et al. 2004; Lea et al. 2006) and from mollusk assemblages (e.g. Sandweiss et al. 1996). In the mid-Holocene, some reconstructions show relative cooling of SSTs in the eastern equatorial Pacific (Koutavas et al. 2002) while other evidence suggests relative warming or little change from present (Lea et al. 2006). There is also evidence that the western equatorial Pacific was more saline in the mid-Holocene according to reconstructions from oxygen isotope ratios in coral (Gagan et al. 1998; Tudhope et al. 2001) and marine sediments (Stott et al. 2004), implying decreased precipitation or increased evaporation. As the mean changes in mid-Holocene equatorial Pacific SST and associated changes in precipitation and atmospheric circulation are not strongly constrained by the available proxy records, we do not identify a specific target mean state to compare with the model simulations.

Records of interannual variability associated with ENSO include laminated lake sediment records of flood events in South America (e.g. Rodbell et al. 1999; Moy et al. 2002). Analysis of the Holocene sediment record indicates that the periodicity of heavy precipitation (El Niño) events has evolved from longer than 15 years prior to 7 ka towards a modern periodicity after 5 ka, implying the onset of modern ENSO between 7–5 ka. Fossil corals from the mid-Holocene have been used to reconstruct ENSO-related SST and salinity variability in the western Pacific (Gagan et al. 1998; Tudhope et al. 2001; Gagan et al. 2004; McGregor and Gagan 2004). Interannual variability of coral oxygen isotope and Sr/Ca ratios at ENSO periods is found to be weaker in mid-Holocene coral than in modern coral from the same site, implying reduced ENSO amplitude. Fossil coral records from the Huon Peninsula, Papua New Guinea (PNG) contain a reduction of 60% in the standard deviation of mid-Holocene oxygen isotope ratios compared with modern records (Tudhope et al. 2001). McGregor and Gagan (2004) report an ENSO amplitude reduction of 15% in fossil coral records from a northern PNG site using a measure based on the average coral isotopic anomaly for El Niño events over a threshold. Gagan et al. (2004) report a reduction of 20% in SST variability and 70% reduction in precipitation variability at ENSO periods in a mid-Holocene coral record from the Great Barrier Reef.

We aim to compare the model simulations of changes in mid-Holocene ENSO with changes in ENSO characteristics inferred from fossil coral records. As different measures are used to calculate changes in ENSO amplitude in each coral study, it is difficult to identify a single target to compare with the model simulations. The study of Tudhope et al. (2001) provides a maximum estimate of 60% reduction in ENSO amplitude in the mid-Holocene, while McGregor and Gagan (2004) calculate a smaller 15% reduction in the amplitude of an average El Niño event. The extent to which these measures can be compared with the standard deviation of central Pacific SST variability is discussed further in a forthcoming study. We assume here a range of 15–60% ENSO amplitude reduction is consistent with the available coral records, while noting that corals record local ENSO SST and precipitation variability, which may not always mirror changes in basin-scale ENSO.

Previous atmosphere-only and coupled model studies of the mid-Holocene include simulations carried out as part of the Palaeoclimate Modelling Intercomparison Project (PMIP) (e.g. Harrison et al. 1998; Braconnot et al. 1999, 2000; Joussaume et al. 1999; Zhao et al. 2005). Previous modelling studies of the sensitivity of ENSO to Holocene orbital forcing using the reduced-complexity Zebiak–Cane model (Zebiak and Cane 1987) identified a reduction in ENSO amplitude in the mid-Holocene (Clement et al. 2000, 2001). Coupled atmosphere–ocean GCM studies have also investigated mid-Holocene tropical climate and ENSO (e.g. Hewitt and Mitchell 1998; Bush 1999; Liu et al. 2000; Kitoh and Murakami 2002; Otto-Bliesner et al. 2003). Those studies that examine ENSO variability report a modest reduction in the amplitude of ENSO in early and mid-Holocene simulations (e.g. Liu et al. 2000; Otto-Bliesner et al. 2003). Some find a relative cooling in the eastern Pacific (Bush 1999; Liu et al. 2000; Otto-Bliesner et al. 2003), while other studies find greater cooling in the central Pacific (Kitoh and Murakami 2002). A preliminary discussion of simulations with the standard version of HadCM3 reported a reduction of 12% in the amplitude of ENSO (as measured by the NINO3 SST index) in the mid-Holocene compared with the pre-industrial simulation, while the mean equatorial Pacific SST gradient was unchanged (Brown et al. 2006).

This study aims to explore uncertainty in model ENSO sensitivity to climate forcing using simulations of pre-industrial and mid-Holocene climate from an ensemble of coupled model versions. We use multiple versions of HadCM3 for which selected parameters in the atmospheric model are perturbed within a plausible, expert-defined range (Murphy et al. 2004; Collins et al. 2006). As this study represents a first attempt to use such a ''perturbed physics'' ensemble to simulate palaeoclimate, we also investigate the impact of seasonally-varying and constant

annual mean heat flux adjustments used to correct the radiative imbalances caused by the perturbations. The mid-Holocene mean climates and ENSO characteristics simulated by the different model versions are compared, and the reasons for changes in ENSO behaviour are considered. The same perturbed physics ensemble members have been used to simulate climate with increasing greenhouse gas concentrations (Collins et al. 2006), and the ENSO sensitivity in these simulations is examined in a forthcoming study. Here we consider how the ability of each model version to simulate mid-Holocene changes in ENSO characteristics could provide one measure for assessing the credibility of model predictions of future changes in ENSO behaviour.

2 Model and experiments

HadCM3 is a coupled atmosphere-ocean model with 3.75° longitude and 2.5° latitude horizontal resolution and 19 levels in the atmosphere (Pope et al. 2000). The ocean component has a uniform resolution of 1.25° with 20 vertical levels (Gordon et al. 2000). The standard model exhibits no significant surface climate drift, and so can perform multi-century integrations without flux adjustments, albeit with regional SST biases. The standard model is run without flux adjustments for pre-industrial (''0K'' run) and mid-Holocene (''6K'' run) climate for 100 years, using initial conditions from previous pre-industrial and mid-Holocene simulations.

The mid-Holocene simulations are forced with the appropriate changes in orbital parameters (Berger 1978), primarily a shift in the timing of perihelion to late August, resulting in changes in the seasonal cycle of insolation. The experimental design follows the PMIP Phase II protocol (see http://www.pmip2.cnrs-gif.fr), with the exception of small differences in the atmospheric concentration of N_2O and the use of pre-industrial methane concentrations for the mid-Holocene run. The atmospheric CO_2 composition is set at pre-industrial values for the mid-Holocene simulation as CO_2 concentrations are known to have been relatively unchanged, while there is evidence that methane concentrations were reduced at this time (Chappallaz et al. 1997). Vegetation coverage is fixed, although previous modelling studies have suggested that interactive climate-vegetation feedbacks may be important for simulating mid-Holocene climate (e.g. Ganopolski et al. 1998). The impact of changes in methane concentration and vegetation coverage is expected to be of second-order importance for ENSO variability. Varying only the orbital forcing allows us to isolate the influence of altered seasonality on ENSO and to compare our results with other modelling studies that have used similar boundary conditions.

Fig. 1 Seasonal cycle of ocean
heat flux adjustments (Wm^{-2})
averaged over 4°N–4°S in the
equatorial Pacific for
a HadCM3.0 seasonally-varying
flux-adjusted runs and
b HadCM3.0A constant flux-
adjusted runs. Values in **b** are
a simple time-average of those
in **a**
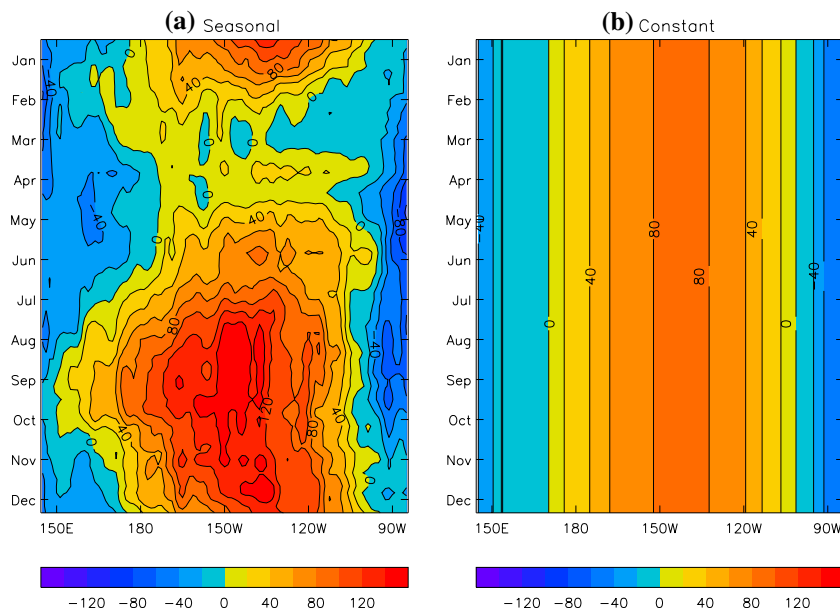
HadCM3 has been shown to simulate ENSO as well as other current generation coupled models, with an amplitude and frequency that is broadly in agreement with observations (e.g. Collins et al. 2001; Latif et al. 2001; AchutaRao and Sperber 2002, 2006; Toniazzo et al. 2007). However, biases in the model climate which may influence ENSO behaviour and sensitivity include a cold SST bias in the central equatorial Pacific Ocean and a warm SST bias over the Maritime Continent, stronger than observed equatorial Pacific trade winds and convection which is too strong and overly confined to the western Pacific warm pool (e.g. Innes et al. 2003; Turner et al. 2005). Although the elimination of flux-adjustment terms from coupled atmosphere-ocean models has been seen as a significant advance, it is at the expense of such biases. For this reason, and because perturbation of model parameters can lead to top-of-the-atmosphere radiation imbalances, we use flux adjustments in the perturbed physics simulations. We also carry out a set of unperturbed model simulations with flux adjustments for comparison.

The method for calculating the flux-adjustment terms is described in detail by Collins et al. (2006). Briefly, a ''Haney forcing'' phase of relaxation to observed SST and salinity is performed for each model version and the fluxes of heat and freshwater are stored and averaged. These fluxes are then applied as a seasonally varying but constant forcing term during the experiments described here. Thus there is no explicit relaxation, which would tend to suppress the variability that is of interest, but regional biases in SST and surface salinity are greatly reduced. In addition, the integrated heat flux adjustment cancels any top-of-the-atmosphere radiation imbalance. As mid-Holocene SST

and salinity climatologies are not known, flux adjustment to pre-industrial values is used for the mid-Holocene simulations. While this may introduce biases in the mid-Holocene climate, these are expected to be smaller than the biases in the uncorrected model climatology or model drift due to radiative imbalance.

Following Collins et al. (2006), the unperturbed model with seasonally varying flux adjustments is labelled ''HadCM3.0'' to distinguish it from the non-flux-adjusted standard version, ''HadCM3''. In addition, because the seasonal cycle of the flux adjustments may interfere with the model response to mid-Holocene seasonal orbital forcing, we include a set of simulations with a constant, annually averaged flux-adjustment term that is applied in the same manner as the seasonally varying adjustment. This experimental set-up is labelled ''HadCM3.0A''. The equatorial Pacific seasonally varying and constant heat flux adjustments for the HadCM3.0 and HadCM3.0A experiments are shown in Fig. 1.

The perturbed physics ensemble members are a subset of 17 (the standard model and 16 perturbed physics versions) from a larger ensemble of 129 atmospheric model versions with multiple parameters and switches perturbed simultaneously as part of the quantifying uncertainties in model prediction (QUMP) project (Murphy et al. 2004; Webb et al. 2006). The combination of parameter settings was chosen to span the range of climate sensitivity as well as to maximise the chance of producing models with adequate base climates. The 17 coupled model versions have been used to simulate pre-industrial climate and transient climate change with 1% per year increasing CO_2 concentrations, as discussed by Collins et al. (2006). A detailed

Table 1 Model experiments

Model	Run	Perturbed?	Flux-adjusted?	Length of run (years)
HadCM3	0K	No	No	100
HadCM3	6K	No	No	100
HadCM3.0	0K	No	Seasonal	100
HadCM3.0	6K	No	Seasonal	100
HadCM3.0A	0K	No	Constant	100
HadCM3.0A	6K	No	Constant	100
HadCM3.1	0K	Yes	Seasonal	100
HadCM3.1	6K	Yes	Seasonal	50
HadCM3.3	0K	Yes	Seasonal	100
HadCM3.3	6K	Yes	Seasonal	50
HadCM3.8	0K	Yes	Seasonal	100
HadCM3.8	6K	Yes	Seasonal	50
HadCM3.13	0K	Yes	Seasonal	100
HadCM3.13	6K	Yes	Seasonal	50

0K pre-industrial, *6K* mid-Holocene

examination of the ENSO characteristics of the perturbed physics models in the pre-industrial simulations is given in the study of Toniazzo et al. (2007).

In this study, a subset of four perturbed physics model versions are used to simulate mid-Holocene climate. We compare these simulations with the corresponding pre-industrial simulations from the QUMP project and therefore adopt the same experimental set-up, including the use of seasonal flux-adjustments, for our mid-Holocene simulations. The four versions were chosen to sample the maximum range of ENSO amplitude in the pre-industrial climate, with one model simulating a very strong ENSO, two versions simulating a very weak ENSO and one version having an ENSO amplitude comparable to observations (HadCM3.1, HadCM3.3, HadCM3.8 and HadCM3.13, as identified by Collins et al. 2006). Each model has 29 atmospheric model parameters simultaneously perturbed, so that the different climates and ENSO characteristics simulated cannot be ascribed to the influence of any one particular parameter. The parameter settings for each perturbed physics ensemble member are described in Collins et al. (2006). The standard, flux-adjusted and perturbed physics model versions and experiments included in this study are listed in Table 1.

3 Mid-Holocene tropical climate

The main features of the time-averaged mid-Holocene climate simulated by each model version are compared in order to determine whether all model versions simulate a plausible mid-Holocene climate, and whether differences between the simulated climates may explain different ENSO sensitivity. The results are presented for the standard model (HadCM3) as well as the unperturbed model versions with seasonally varying and constant flux adjustments (HadCM3.0 and HadCM3.0A). Results for the perturbed physics model versions are discussed briefly as the large-scale mid-Holocene climate anomalies are broadly similar to the results for unperturbed flux-adjusted runs.

3.1 Surface temperature

The change in seasonal average (December–January–February, DJF, and June–July–August, JJA) surface temperature from pre-industrial to mid-Holocene climate is shown for HadCM3, HadCM3.0 and HadCM3.0A model runs in Fig. 2. The mid-Holocene anomalies in the seasonal cycle of SST on the equator (averaged over 4°N–4°S) for the same model runs are shown in Fig. 3. Consistent with reduced insolation during DJF in the mid-Holocene (cooler boreal winter and austral summer), all model versions simulate predominantly cooler continental surface temperatures in the tropics and mid-latitudes. In response to the positive mid-Holocene insolation anomaly in JJA, all models simulate warmer tropical and mid-latitudes continental surface temperatures with the exception of local cooling over South Asia and tropical North Africa, associated with increased Asian and North African monsoon precipitation. The large-scale surface temperature anomalies for the perturbed physics model versions (HadCM3.1 etc., not shown) are similar to the seasonally varying flux-adjusted (HadCM3.0) runs.

In DJF, the spatial pattern of cooling of tropical Pacific SSTs is somewhat La Niña-like in the standard and flux-adjusted runs, with greater cooling in the eastern Pacific and warming confined to the western Pacific warm pool and subtropics. The tropical Pacific is also cooler in JJA in the mid-Holocene, despite the positive insolation anomaly, with the exception of local warming in the eastern equatorial Pacific (standard model runs) and central equatorial Pacific (flux-adjusted and perturbed physics runs). All model versions simulate larger temperature anomalies in the eastern Pacific than the western Pacific despite being forced by a zonally uniform insolation anomaly, indicating the role of local atmosphere-ocean feedbacks in controlling SSTs.

The zonal cross section of annual mean mid-Holocene Pacific SST anomalies, averaged over 4°N–4°S, is shown in Fig. 4. Modelled annual mean tropical SSTs are generally cooler in the mid-Holocene, in response to reduced annual mean insolation over the tropics. While cooling of central and eastern equatorial Pacific SSTs occurs in all unperturbed mid-Holocene model runs, western Pacific

Fig. 2 Differences between
mid-Holocene and pre-
industrial average DJF (*left*) and
JJA (*right*) surface temperature
(°C) for **a**, **b** HadCM3,
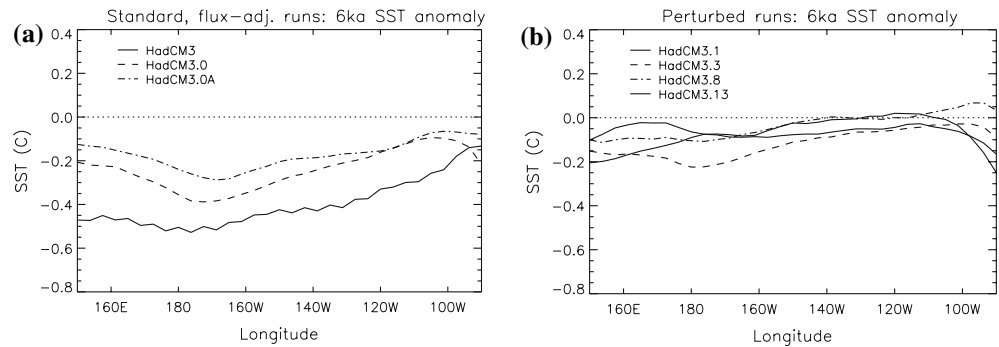**c**, **d** HadCM3.0 and
e, **f** HadCM3.0A simulations
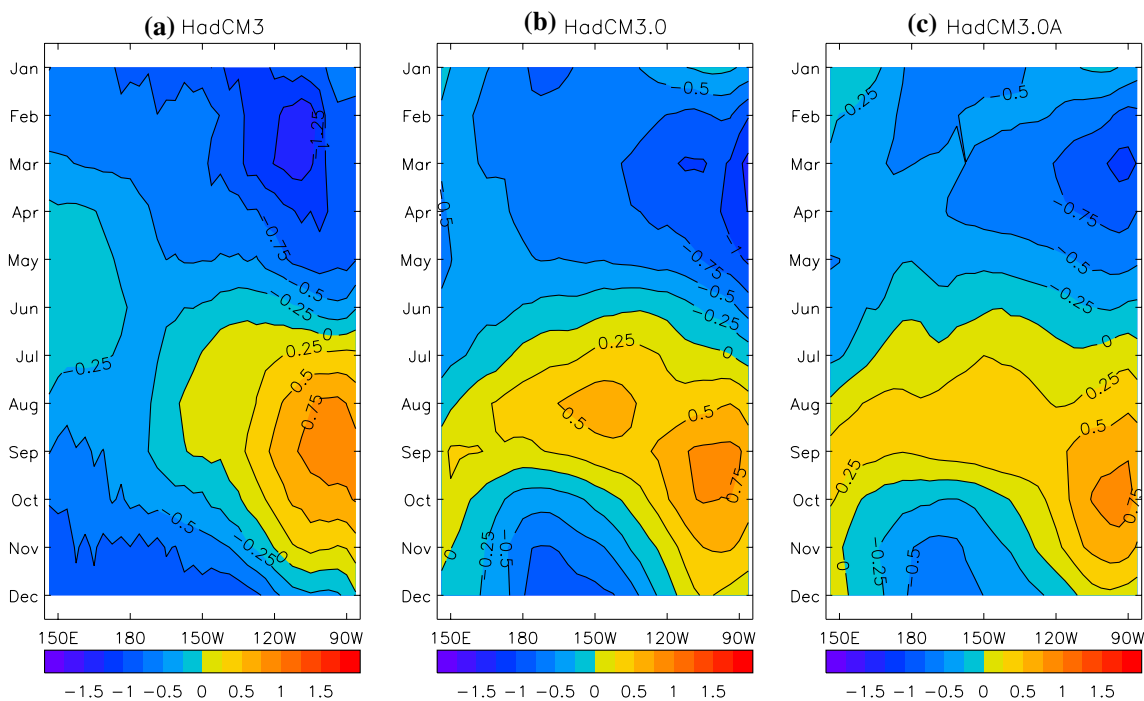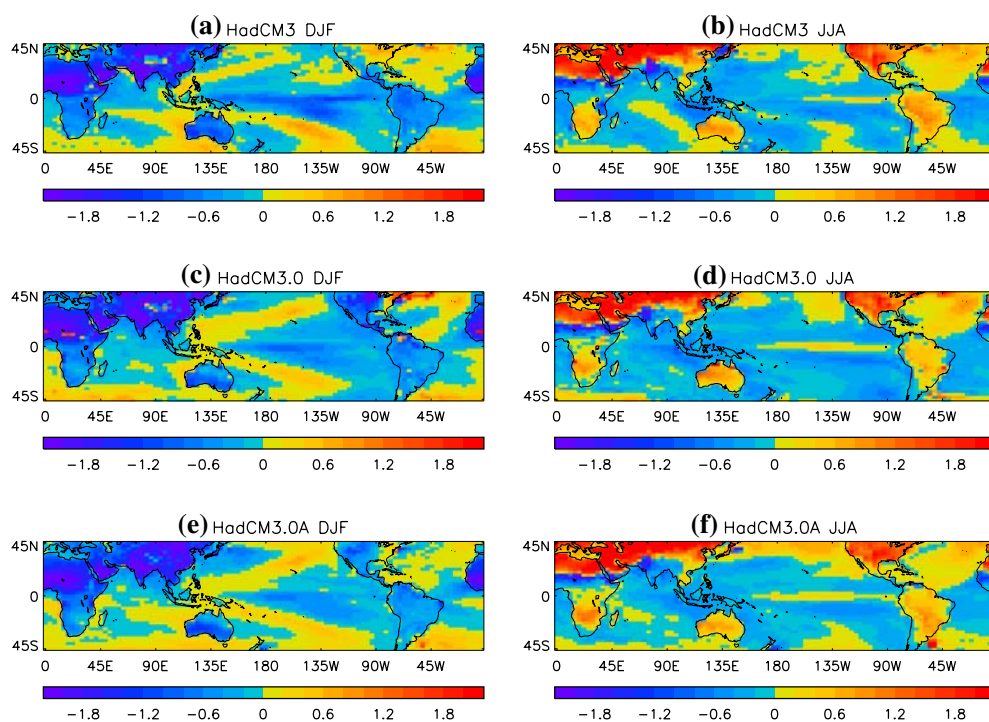
Fig. 3 Differences between seasonal cycle of mid-Holocene and pre-industrial SST (°C) averaged over 4°N–4°S in the equatorial Pacific for **a** HadCM3, **b** HadCM3.0 and **c** HadCM3.0A simulations

SSTs also experience cooling of the same or larger magnitude. The standard model version simulates a slightly reduced annual mean zonal SST gradient due to the warming in the eastern Pacific from July to November, as shown in Fig. 3. The annual mean equatorial zonal SST gradient is unchanged to within ±0.2°C in the flux-adjusted HadCM3.0 and HadCM3.0A simulations (Fig. 4a) and in the perturbed physics simulations

Fig. 4 Differences between mid-Holocene and pre-industrial annual mean SST (°C) averaged over 4°N–4°S for **a** HadCM3, HadCM3.0 and HadCM3.0A simulations and **b** perturbed physics simulations

Fig. 5 Differences between mid-Holocene and pre-industrial DJF (*left*) and JJA (*right*) precipitation (mm/day) for **a**, **b** HadCM3, **c**, **d** HadCM3.0 and **e**, **f** HadCM3.0A simulations
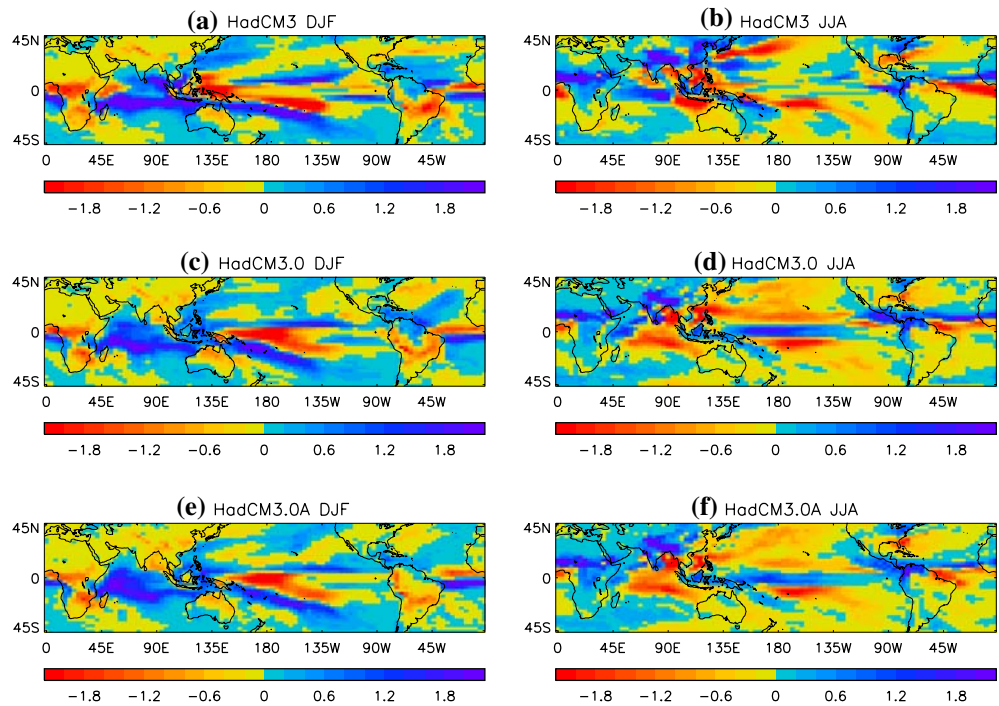
(Fig. 4b). Therefore, the simulated annual mean tropical Pacific SSTs cannot be described as La Niña-like in any of the mid-Holocene simulations, in disagreement with previous coupled model studies discussed in Sect. 1.
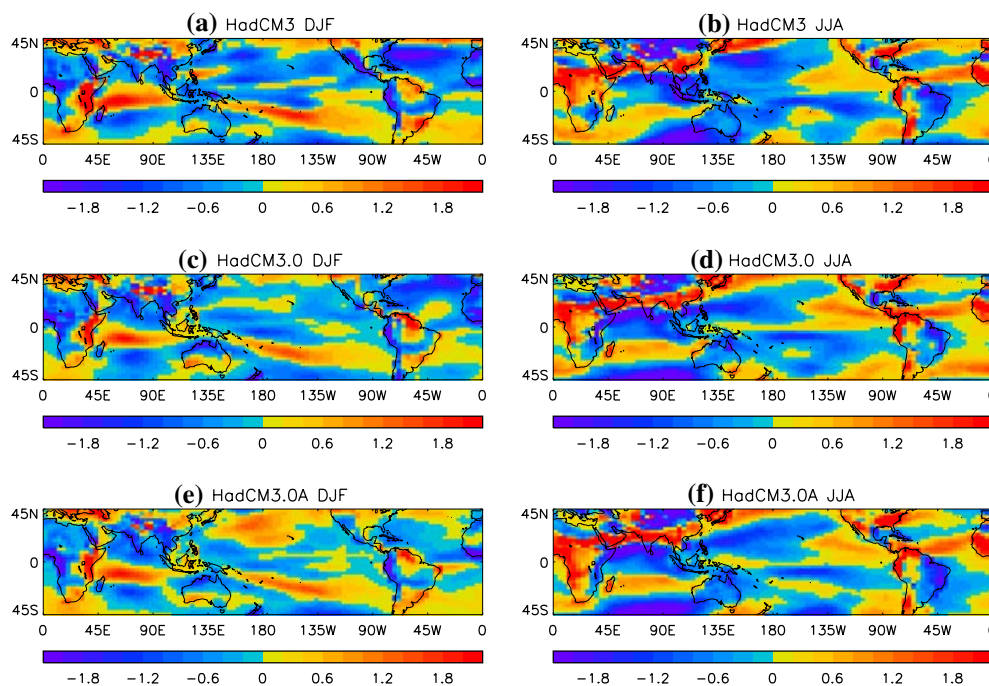
3.2 Precipitation

The mid-Holocene DJF and JJA seasonal precipitation anomalies for the HadCM3, HadCM3.0 and HadCM3.0A simulations are shown in Fig. 5. In DJF, precipitation is reduced in the western and central tropical Pacific and increased over the Indian Ocean in all simulations. Precipitation associated with the south Pacific convergence zone (SPCZ) is intensified and shifted southward. The DJF tropical Pacific precipitation anomalies resemble precipitation anomalies during a La Niña event, consistent with the simulated DJF SST anomalies. The DJF precipitation anomalies in the perturbed physics runs are similar to the

HadCM3.0 anomalies, with an intensified SPCZ and reduced precipitation in the central-western equatorial Pacific in all cases (not shown).

In JJA, the Asian and North African summer monsoons are stronger in the mid-Holocene for all model versions due to increased NH seasonality and land–ocean temperature gradients. The strengthening of Asian and North African summer monsoons is a direct response to the change in insolation, as a similar response was identified in the PMIP atmosphere-only GCM simulations (Joussaume et al. 1999). The northern Australian summer (DJF) monsoon is enhanced in all mid-Holocene simulations, in agreement with Liu et al. (2004), who found that ocean feedbacks produced a stronger northern Australian monsoon in coupled model simulations. South American summer monsoon precipitation is reduced in the mid-Holocene for all model versions in response to reduced insolation during DJF, again in agreement with Liu et al. (2004). The North

Fig. 6 Differences between mid-Holocene and pre-industrial DJF (left) and JJA (right) zonal wind stress ($Nm^{-2} \times 100$) for a, b HadCM3, c, d HadCM3.0 and e, f HadCM3.0A simulations

American summer monsoon is weaker in the HadCM3 mid-Holocene simulation, but stronger in the flux-adjusted simulations, showing the influence of the mean state on the monsoon response.

Precipitation is increased in JJA in the western and central tropical Pacific in the flux-adjusted and perturbed physics mid-Holocene simulations, whereas increased precipitation in JJA is confined to the Maritime Continent and SPCZ region in the standard model run. The inter-tropical convergence zone (ITCZ) travels further north in JJA and further south in DJF in the Atlantic sector in all mid-Holocene simulations, with an annual mean northward shift in the flux-adjusted runs consistent with evidence from Cariaco Basin sediment records for a more northerly Atlantic ITCZ in the early and mid-Holocene (Haug et al. 2001). A boreal summer and annual mean northward ITCZ shift over the eastern Pacific is only evident in the flux-adjusted simulations. Western Pacific seasonal and annual mean mid-Holocene precipitation anomalies are more spatially complex and do not consist of a clear meridional displacement of the ITCZ in any case.

3.3 Zonal wind stress

The mid-Holocene DJF and JJA seasonal zonal wind stress anomalies for the HadCM3, HadCM3.0 and HadCM3.0A model simulations are shown in Fig. 6 and the change in the seasonal cycle of zonal wind stress in the equatorial Pacific is shown in Fig. 7. Negative zonal wind stress anomalies over the Pacific represent an intensification of easterly trade winds. In DJF, the easterly trade winds are

stronger in the western and central equatorial Pacific and weaker in the eastern Pacific in all the mid-Holocene simulations. All model versions simulate a mid-Holocene increase in the seasonal relaxation of the trade winds during boreal spring in the tropical western Pacific. During JJA, stronger trade winds are simulated in the western and central equatorial Pacific in the HadCM3 6K run. Stronger western and central Pacific trade winds develop in the flux-adjusted and perturbed physics (not shown) 6K runs slightly later, during boreal autumn. The stronger trade winds do not extend to the eastern equatorial Pacific, where positive zonal wind stress anomalies (i.e. weaker easterly winds) are seen in all 6K model runs in July–September, with larger anomalies in the flux-adjusted simulations.

The atmospheric circulation response to mid-Holocene forcing simulated by all model versions differs from previous studies which found strengthened annual mean or boreal summer trade winds across the tropical Pacific, contributing to a cooling of eastern Pacific SSTs (e.g. Bush 1999; Liu et al. 2000; Otto-Bliesner et al. 2003). The stronger Asian summer monsoon circulation over the Maritime Continent appears to be driving enhanced western Pacific trade winds from June onwards in the HadCM3 6K simulation and from August onwards in the flux-adjusted simulations, while zonal wind stress changes in the eastern Pacific appear to be controlled by local atmosphere-ocean feedbacks.

3.4 Upper ocean temperature

The amplitude of ENSO may be influenced by changes in the upper ocean thermal structure, including changes in the
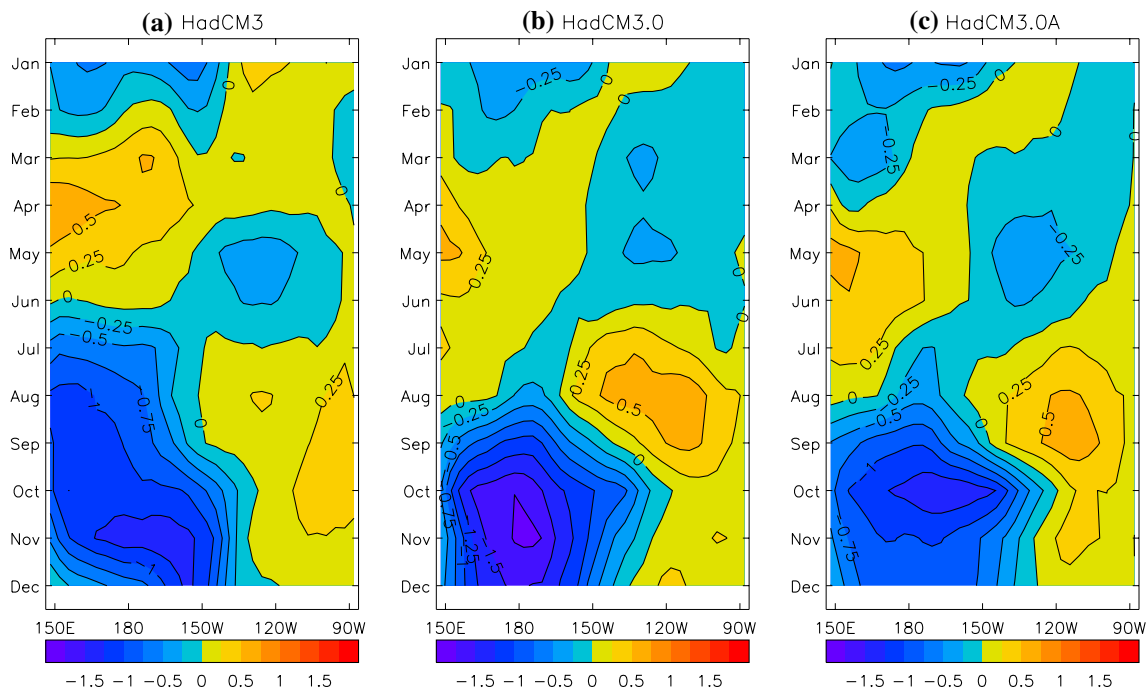
Fig. 7 Differences between seasonal cycle of mid-Holocene and pre-industrial zonal wind stress ($Nm^{-2} \times 100$) averaged over 4°N–4°S in the equatorial Pacific for **a** HadCM3, **b** HadCM3.0 and **c** HadCM3.0A simulations

depth and intensity of the thermocline (e.g. Meehl et al. 2001). The coupled model study of Liu et al. (2000) identified a weakening of the equatorial Pacific tropical thermocline as a cause of reduced ENSO amplitude in mid-Holocene simulations. The mid-Holocene changes in annual mean upper ocean temperature in the equatorial Pacific for the HadCM3, HadCM3.0 and HadCM3.0A runs are shown in Fig. 8, with the 20°C isotherm shown for both 0K and 6K runs. In all simulations, the surface water is cooler across the equatorial Pacific, with a weak local subsurface warming in the far eastern Pacific in the flux-adjusted runs. The surface cooling and subsurface warming in the central–eastern Pacific results in a modest mid-Holocene weakening of equatorial thermocline intensity in all cases, with the largest weakening occurring in the HadCM3 simulations.

The thermocline intensity is calculated from the vertical distance between the 22°C isotherm and the 16°C isotherm on the equator at 155°W (Meehl et al. 2001). By this measure, the eastern Pacific equatorial thermocline is less intense in the HadCM3 6K run than the 0K run (59 m at 0K, 72 m at 6K), while the intensity is almost unchanged for the HadCM3.0 runs (57 m at 0K, 53 m at 6K), and the HadCM3.0A runs (60 m at 0K, 63 m at 6K). The depth of the thermocline, as measured by the equatorial 20°C isotherm depth at 155°W, is changed in the mid-Holocene by less than 1 m for all three-model versions. However the slope of the thermocline is slightly increased in the Had-

CM3 6K run, due to a deeper western Pacific thermocline and shoaling of the eastern Pacific thermocline. The thermocline intensity and depth are unchanged within the same range in the perturbed physics runs (not shown).

3.5 Comparison of model versions

In broad terms, the standard, flux-adjusted and perturbed physics model versions produce similar large-scale responses to mid-Holocene orbital forcing. That is, they all show boreal winter continental cooling, summer continental warming and enhanced Asian and North African summer monsoon circulations, reduced-strength trade winds in spring and strengthened trade winds in autumn. Thus the flux adjustments and parameter perturbations appear to have no leading-order impact on the large-scale response to mid-Holocene orbital forcing.

However, there are some differences in the details of the response, which could potentially have an impact on the sensitivity of ENSO characteristics to changes in climate forcing. The mid-Holocene changes in zonal wind stress differ in the flux-adjusted and perturbed physics simulations, with a delay in the summer–autumn enhancement of the easterly trade winds in the central and western Pacific. The seasonal changes in equatorial Pacific SSTs also differ, with a boreal summer warming confined to the eastern Pacific in the standard model 6K run but extending to the central and western Pacific in the flux-adjusted simulations.
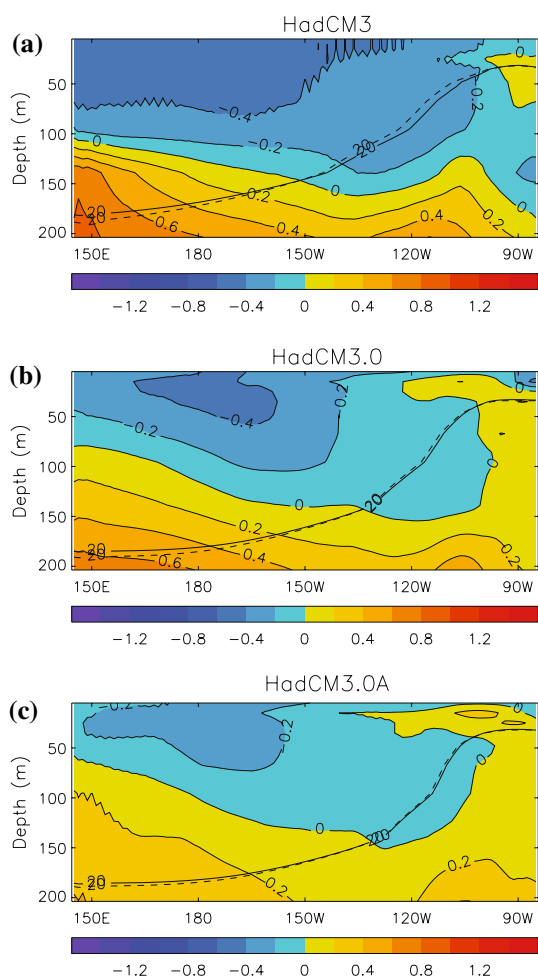
Fig. 8 Differences between mid-Holocene and pre-industrial annual mean upper ocean temperature (top 200 m), averaged over 2°N–2°S, for **a** HadCM3, **b** HadCM3.0 and **c** HadCM3.0A simulations. The 20°C isotherm for the pre-industrial (*solid line*) and mid-Holocene (*dashed line*) runs are also shown

There are also some differences between changes in the intensity of the central and eastern Pacific equatorial thermocline, with a greater reduction in thermocline intensity due to subsurface warming and surface cooling in the standard model simulations.

Attempts to determine which simulation is more plausible by quantitative evaluation of the model response against the sparse network of palaeo-records are limited by the local biases in the standard model, and by the use of flux adjustments in the other simulations. A local-scale comparison with palaeoclimate proxy records requires that the model correctly simulates regional climate and teleconnections, such as interactions between the Asian monsoon and ENSO and regional precipitation responses to ENSO in the western Pacific warm pool. Previous studies have found that the use of heat flux adjustment reduces the influence of SST biases in the mean climate of HadCM3, which can greatly improve the simulation of ENSO–mon-

soon interactions and ENSO teleconnections (e.g. Turner et al. 2005). However such flux adjustments may also strongly perturb the atmosphere–ocean feedbacks in the tropical Pacific (e.g. Spencer et al. 2007) which are likely to be important for the response of ENSO to mid-Holocene orbital changes. Therefore, the flux-adjusted model which simulates the most realistic present-day mean climate (and seasonal cycle) may not simulate the most realistic response to palaeoclimate forcing, particularly for a mode of variability such as ENSO which results from nonlinear interactions between the atmosphere and ocean.

4 Mid-Holocene ENSO

The spatial pattern of interannual SST variability, shown in Fig. 9, is compared for each model run to determine the region of maximum interannual variability associated with ENSO. The largest interannual SST variability in the standard HadCM3 runs is located in the NINO3 region (5°S–5°N, 90°W–150°W), whereas the largest variability in the flux-adjusted and perturbed physics runs is located slightly further west in the NINO3.4 region (5°S–5°N, 120°W–170°W), a common feature in flux-adjusted versions of HadCM3 (Spencer et al. 2007).

In this study, we use monthly SST anomalies in the NINO3 region (NINO3 index) as a measure of ENSO activity, as the response to mid-Holocene forcing is similar using NINO3 or NINO3.4 indices. The spatial patterns of SST variability do not differ significantly between pre-industrial and mid-Holocene simulations, in contrast with a zonal displacement of the maximum ENSO SST anomalies observed in HadCM3 simulations of Last Glacial Maximum and increased greenhouse gas climates (Toniazzo 2006).

4.1 ENSO amplitude and frequency

The timeseries of NINO3 SST anomalies for mid-Holocene and pre-industrial runs with all model versions are shown in Fig. 10, with the standard deviation of the NINO3 timeseries included in the top left corner of the plots. As outlined by Brown et al. (2006), the standard model version (HadCM3) simulates a 12% reduction in ENSO amplitude, as measured from the NINO3 standard deviation, in the mid-Holocene climate. While this difference in amplitude is within the range of internal model variability for 100-year segments of a 1,000-year HadCM3 control run (Collins 2000), it is of the same magnitude as mid-Holocene ENSO amplitude reduction reported in other coupled model studies (e.g. Liu et al. 2000; Otto-Bliesner et al. 2003). The seasonally flux-adjusted model simulates an increase in ENSO amplitude in the mid-Holocene (+4%),

Fig. 9 Standard deviation of
monthly anomalies of SST (°C)
for **a** HadCM3 0K, **b** HadCM3
6K, **c** HadCM3.0 0K,
d HadCM3.0 6K,
e HadCM3.0A 0K,
f HadCM3.0A 6K simulations
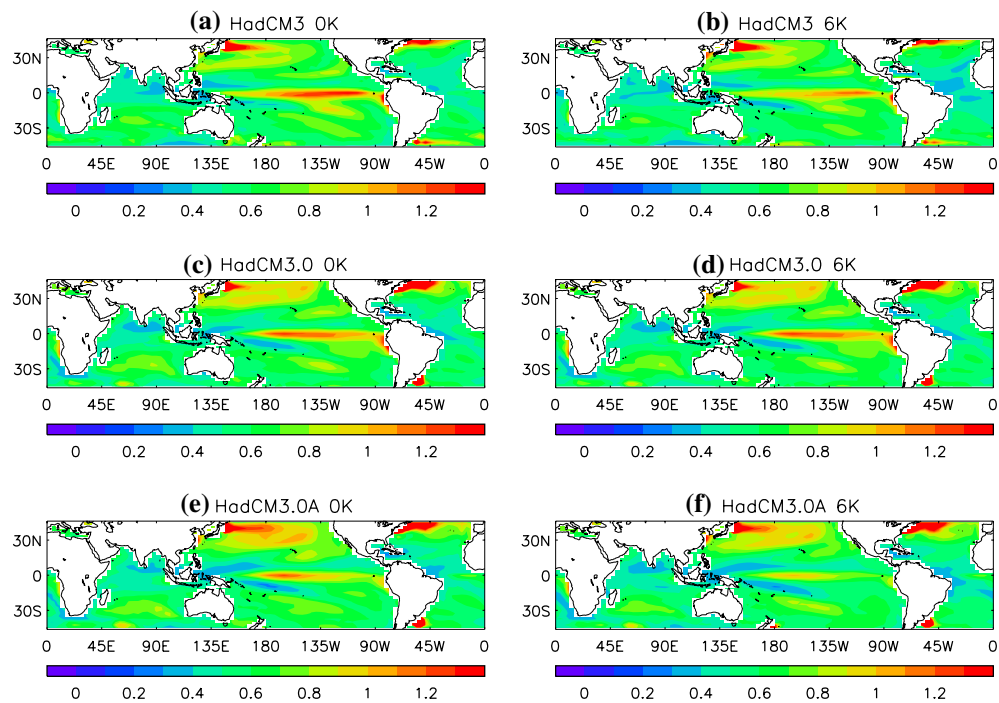
which is clearly inconsistent with both proxy records and previous modelling studies. The constant flux-adjusted model simulates a 14% reduction in ENSO amplitude, which is comparable to the standard model runs. These results suggest that the use of ocean heat flux-adjustments with a modern seasonal cycle alters the response of ENSO in HadCM3 to mid-Holocene orbital forcing, a result which will be discussed further below.

The perturbed physics model versions have a range of ENSO amplitudes, from around 50% weaker to around 50% stronger than standard HadCM3 in the pre-industrial runs, as shown in Fig. 10. A detailed analysis of the reasons for the different ENSO characteristics of the perturbed model versions is given by Toniazzo et al. (2007), while this study focuses on the sensitivity of the model ENSO to mid-Holocene orbital forcing. The perturbed physics model versions simulate an increase in ENSO amplitude in the 6K runs for all four perturbed models (+18, +6, +19 and +10% respectively), as for the seasonally flux-adjusted HadCM3.0 runs. It appears that the use of seasonally varying flux adjustment in the perturbed physics simulations has altered the response to mid-Holocene forcing in a similar manner to the HadCM3.0 simulations. While the short (50-year) length of the perturbed physics 6K runs increases the chance of sampling biases, the common response of all the seasonally flux-adjusted model versions suggests that the result is a robust feature of this model configuration.

Changes in the frequency of ENSO are investigated using power spectra of NINO3 SST anomalies calculated for the standard and HadCM3.0 and HadCM3.0A flux-

adjusted 0K and 6K runs, as shown in Fig. 11. The statistical significance of changes in period between the 0K and 6K simulations is estimated using an *f*-test, indicated on the figures. The standard model simulates maximum power at periods of 2–3 and 4–5 years for the pre-industrial climate, while the maximum power in the mid-Holocene simulation is at slightly longer periods of 4–6 years. Both simulations fall within the range of observed modern ENSO periodicity (e.g. AchutaRao and Sperber 2002), and the difference in mid-Holocene ENSO frequency is not statistically significant at the 95% confidence level. In the case of the flux-adjusted simulations, there is a statistically significant reduction in variability at around 6–8 years in the HadCM3.0A 6K run. There is also a statistically significant increase in variability at 6–8 years in the HadCM3.8 6K run (not shown), but changes for the other perturbed physics runs are not significant. Despite these formal statistical estimates of significance, it is difficult to make robust conclusions regarding changes in frequency due to the relatively short length (50–100 years) of the integrations.

The palaeoclimate lake sediment records of Rodbell et al. (1999) suggest that the frequency of strong El Niño events was lower than the modern frequency in the early to mid-Holocene. As the lake sediment record only includes events exceeding a threshold sufficient to produce local flooding, whereas NINO3 SST variability includes information about all warm and cold ENSO events, the model ENSO frequency may not be directly comparable with the lake sediment record. Given the wide range of simulated changes in period for the different model versions, and the

Fig. 10 NINO3 SST anomaly timeseries for **a** HadCM3 0K, **b** HadCM3 6K, **c** HadCM3.0 0K, **d** HadCM3.0 6K, **e** HadCM3.0A 0K, **f** HadCM3.0A 6K, **g** HadCM3.1 0K, **h** HadCM3.1 6K, **i** HadCM3.3 0K, **j** HadCM3.3 6K, **k** HadCM3.8 0K, **l** HadCM3.8 6K, **m** HadCM3.13 0K and **n** HadCM3.13 6K simulations. Standard deviation of NINO3 SST anomalies is shown in top left corner of plots. *Dashed lines* indicate ±2 standard deviations
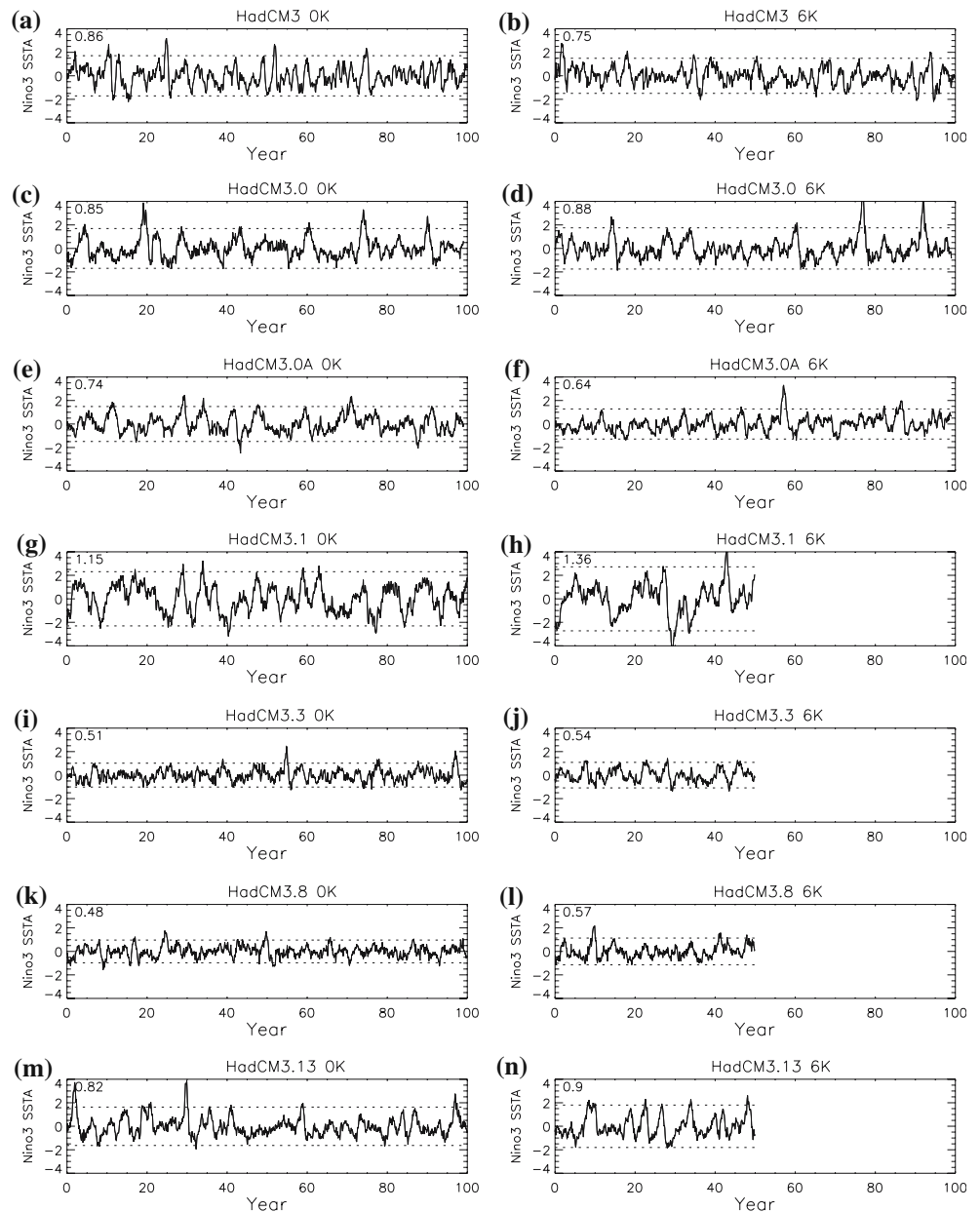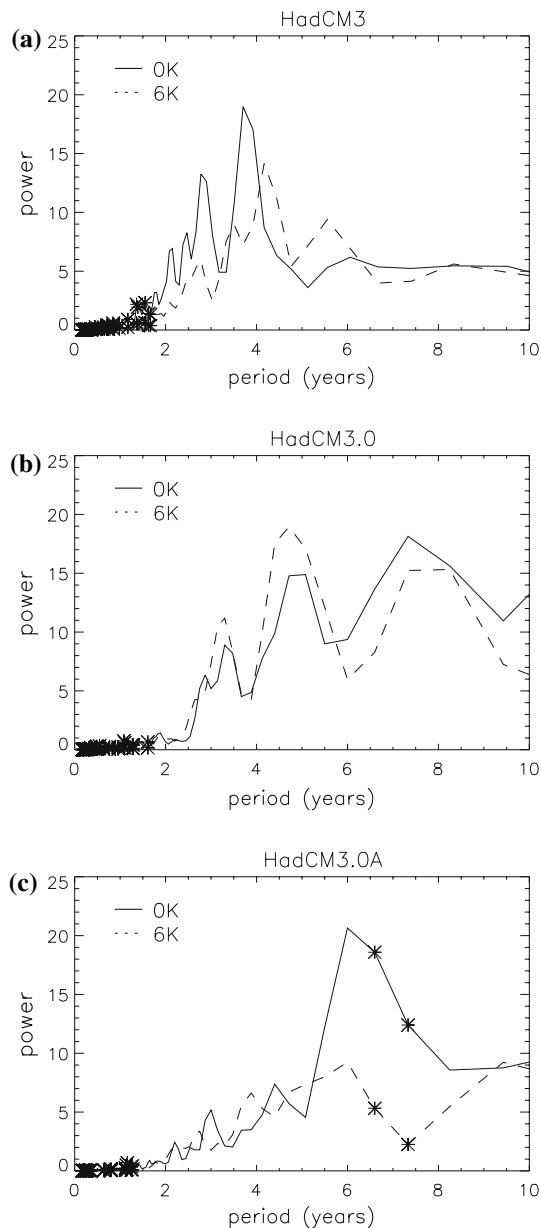

lack of statistical significance in most cases, our results do not conclusively support an interpretation of longer period ENSO variability in the mid-Holocene.

4.2 ENSO and the mean state

Previous studies have proposed that ENSO characteristics may be modulated by changes in the mean state of the tropics, including the mean depth of the equatorial thermocline and the mean strength of the trade winds on the equator. Fedorov and Philander (2000) predict that a reduced ENSO frequency in the early to mid-Holocene should be accompanied by a deeper thermocline, more intense trade winds and a cooler eastern Pacific compared

with present-day climate. In general, the mid-Holocene changes in both mean state and ENSO amplitude in the standard model runs are modest compared with the differences between regimes described by Fedorov and Philander (2000), while the changes in the flux-adjusted and perturbed physics simulations are smaller still. The annual mean thermocline depth (measured from the 20°C isotherm) is slightly deeper in the western Pacific and shallower in the eastern Pacific in the standard model runs, as discussed above, with a negligible change (less than 1 m) in the depth averaged across the equatorial Pacific in all runs. There is a small increase (up to 5%) in annual mean zonal wind stress on the equator in the standard and flux-adjusted mid-Holocene runs, but the changes in zonal

Fig. 11 Power spectra of NINO3 SST anomalies for **a** HadCM3, **b** HadCM3.0 and **c** HadCM3.0A for 0K (*solid line*) and 6K (*dashed line*) runs. *Stars* denote statistically different spectra at the 95% confidence level according to an *f*-test

tending to peak towards the end of the calendar year. As mid-Holocene orbital forcing results in a redistribution of seasonal solar heating in the tropics, we investigate changes to the timing and strength of modelled ENSO–seasonal cycle interactions. The phase-locking of ENSO amplitude to the seasonal cycle is quantified using the monthly standard deviation of NINO3 SST anomalies. The seasonal cycle of NINO3 SST anomalies for each unperturbed model version is shown in Fig. 12, as well as the observed seasonal cycle calculated from HadISST SST data for 1947–2002 (Rayner et al. 2003). The HadCM3 0K run ENSO amplitude has a maximum in December in agreement with observations and a minimum in July, later than the observed April minimum. The HadCM3 6K simulation has reduced seasonal phase-locking, with reduced ENSO amplitude in boreal autumn and winter (the reduction is statistically significant at the 95% confidence level according to an *f*-test). This is broadly consistent with previous studies (e.g. Clement et al. 2000), which find a damping of El Niño SST anomalies from the end of boreal summer in the mid-Holocene.

In the case of the HadCM3.0 runs, the NINO3 SST anomalies are largest at the end of the calendar year and smallest around April as observed, although the SST anomalies do not appear to grow from boreal summer onwards as in observations and the standard 0K run. The strength of ENSO seasonal phase-locking is unchanged in the HadCM3.0 6K run, consistent with the unchanged ENSO amplitude in this run. In the HadCM3.0A pre-industrial simulation, ENSO phase-locking is much weaker than observed and there is no clear maximum in boreal winter. NINO3 SST anomalies are reduced for all months in the mid-Holocene simulation, with no clear phase-locking of ENSO to the seasonal cycle. The seasonal phase-locking of ENSO is also relatively weak in the perturbed physics simulations, with no significant difference between pre-industrial and mid-Holocene simulations (not shown). It appears that imposing a seasonally-varying ocean heat flux adjustment damps seasonal variability in the amplitude of ENSO SST anomalies, which may contribute to the reduced sensitivity of ENSO to mid-Holocene orbital forcing in these simulations.

4.4 ENSO–monsoon interactions

The Asian summer monsoon is enhanced in all mid-Holocene simulations due to increased NH seasonality driving stronger summer land–ocean temperature gradients, as discussed above, producing an increase in summer monsoon precipitation over the Indian subcontinent of up to 20–30%. An increase in Asian summer monsoon strength in the mid-Holocene is also seen in other modelling studies and inferred from palaeoclimate proxy records

wind stress are spatially and temporally variable and do not result in annual mean cooling in the eastern Pacific. It is suggested that seasonal changes in zonal wind stress and thermocline structure play a more important role in determining the response of the model ENSO to mid-Holocene forcing than changes in the annual mean state.
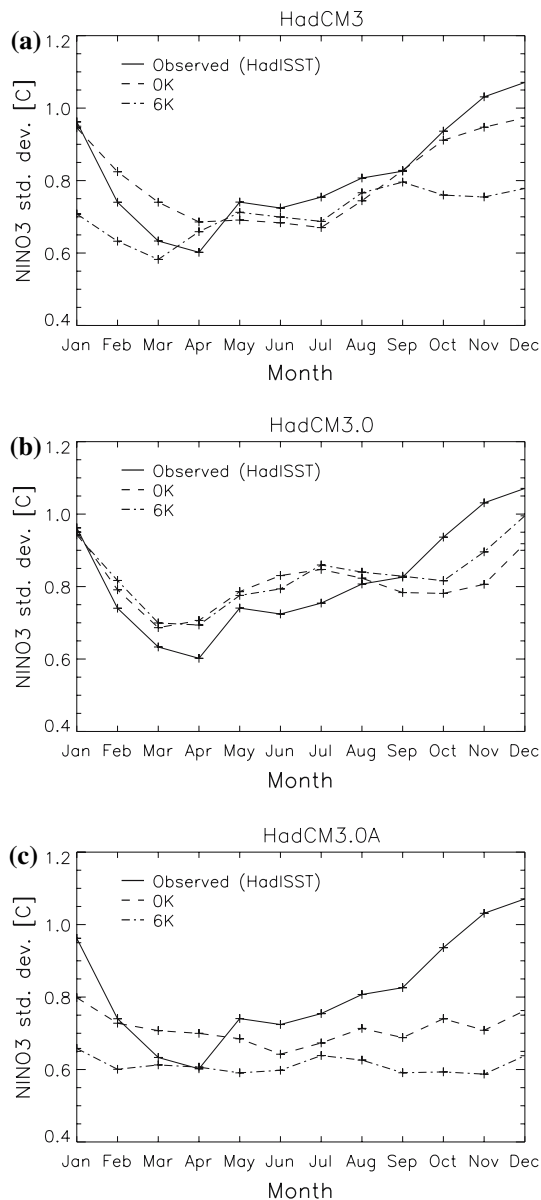
4.3 ENSO seasonal phase-locking

The phase-locking of ENSO to the seasonal cycle is a well known feature of observed ENSO behaviour, with events

Fig. 12 Annual cycle of NINO3 standard deviation for HadISST observations (*solid line*), 0K runs (*dashed line*) and 6K runs (*dot dashed line*) for **a** HadCM3, **b** HadCM3.0 and **c** HadCM3.0A model versions. The difference in NINO3 standard deviation between the HadCM3 0K and 6K runs in boreal winter is statistically significant at the 95% confidence level according to an *f*-test. The flux-adjusted models do not simulate significant changes in monthly NINO3 standard deviation between 0K and 6K runs

of vegetation distribution and lake levels (e.g. Liu et al. 2003; 2004). As the Asian monsoon interacts with ENSO in the modern climate (e.g. Webster and Yang 1992), changes in the strength of the monsoon may play a role in altering mid-Holocene ENSO behaviour. Previous studies have identified the influence of a stronger Asian monsoon driving stronger Pacific trade winds in boreal summer, leading to a damping of El Niño SST anomalies (Liu et al.

2000). A similar boreal summer strengthening of the trade winds in the western equatorial Pacific is seen in the standard HadCM3 mid-Holocene run, and is followed by a damping of positive SST anomalies in this simulation. While the Asian summer monsoon is also enhanced in the flux-adjusted 6K runs, the strengthening of western Pacific trade winds occurs several months later and therefore SST anomalies are not damped to the same extent.

Changes in the interannual variability of monsoon strength may also influence ENSO. The correlation between NINO3 SST anomalies and June–September all india rainfall (AIR) calculated over 60°E–120°E, 10°N–30°N is used to estimate the strength of the tele-connections between the Asian monsoon and ENSO. The correlation is negative in all simulations, indicating stronger monsoons during La Niña conditions, in agreement with the observed ENSO–monsoon relationship (e.g. Webster and Yang 1992). In the standard model simulations, the maximum lagged NINO3–AIR correlation is –0.38 in the 0K run and –0.48 in the 6K run, indicating that there is a stronger ENSO–monsoon interaction in the mid-Holocene simulation. The strength of the ENSO–monsoon interaction is slightly increased in the Had-CM3.0 6K run compared with the 0K run ($r = –0.25$ at 0K, $r = –0.33$ at 6K). In the HadCM3.0A simulations the correlation is strongest in the 0K run ($r = –0.53$ at 0K, $r = –0.16$ at 6K). This may reflect the relative weakness of ENSO in the HadCM3.0A 6K simulation, resulting in little influence of a weak ENSO on a strongly insolation-driven monsoon. The changes are smaller but of the same sign when the dynamical monsoon index of Webster and Yang (1992) is used (not shown).

5 Discussion and conclusions

This study represents the first attempt to use an ensemble of perturbed physics model versions to simulate palaeo-ENSO and investigate model uncertainty in ENSO sensitivity to climate change. As reconstructions from proxy records imply a large reduction in ENSO amplitude in the mid-Holocene, the ability of coupled models to simulate such a response to mid-Holocene forcing constitutes a test of model ENSO sensitivity. Models which simulate a reduced ENSO amplitude (within some range inferred from proxy records) can be considered to have a plausible ENSO sensitivity to climate forcing, providing credibility for simulations of future climate. Formally, the degree of agreement between model and palaeo-data for members of an ensemble of models or perturbed physics model versions can be used to provide weightings for the construction of probabilistic future ENSO predictions (e.g. Murphy et al. 2004; Collins et al. 2006).

In this study, mid-Holocene and pre-industrial climates were simulated with the standard HadCM3 model, model versions with seasonally varying and constant flux adjustment, and four model versions with perturbed atmospheric parameters. In all experiments, mid-Holocene orbital forcing results in changes in tropical surface temperatures and precipitation, which are broadly consistent with palaeoclimate records, including strengthened Asian and North African summer monsoons. The flux-adjusted and perturbed physics model versions simulate mid-Holocene climate anomalies which differ in some respects from the standard model, including simulating warming in the central-eastern equatorial Pacific in boreal summer and precipitation anomalies centred around the dateline rather than over the Maritime Continent. The flux-adjusted model versions also simulate differing changes in the seasonal cycles of SST and zonal wind stress in the tropical Pacific in response to mid-Holocene seasonal insolation anomalies. The different mid-Holocene seasonal cycles lead to changes in the interaction of ENSO SST anomalies with the mean state, contributing to the lack of sensitivity of ENSO to mid-Holocene forcing in the experiments using seasonally varying flux adjustments.

The unchanged or slightly reduced mid-Holocene equatorial Pacific zonal SST gradients simulated in this study differ from the cooler eastern–central Pacific and increased zonal SST gradient found in some previous modelling studies (e.g. Bush 1999; Liu et al. 2000; Otto-Bliesner et al. 2003) and palaeoclimate reconstructions (e.g. Koutavas et al. 2002). The standard model simulates a small relative warming in the eastern equatorial Pacific, while the flux-adjusted models simulate no change in the mean equatorial zonal SST gradient. We also note that the standard HadCM3 simulates larger SST anomalies in the eastern Pacific than in the western Pacific, with insolation-driven warming in boreal summer and cooling in boreal winter in the eastern Pacific. This is in contrast with other intermediate and coupled models (Clement et al. 2000; Liu et al. 2000; Otto-Bliesner et al. 2003), which simulate a boreal summer intensification of the trade winds and cooling in the central–eastern Pacific via Bjerknes feedbacks. As there remains some uncertainty in reconstructions of the mid-Holocene zonal SST gradient from marine sediment records (e.g. Lea et al. 2006), we cannot determine conclusively which model simulation is more plausible. The model-dependence of changes in the equatorial Pacific zonal SST gradient is also seen in increased greenhouse gas simulations (Collins et al. 2005), suggesting that palaeoclimate simulations may play a role in determining which models are more credible, provided sufficient proxy data is available to validate the simulations.

The standard HadCM3 model simulates a 12% reduction in ENSO amplitude in response to mid-Holocene orbital forcing, while the constant flux-adjusted version simulates a 14% reduction, of similar magnitude to previous coupled model studies. The model response in both cases is smaller than the range of reductions in ENSO amplitude of 15–60% inferred from coral proxy records, outlined in Sect. 1. The disagreement between model and coral records may be due to mid-Holocene changes in the strength of ENSO precipitation teleconnections over the western Pacific, amplifying the apparent reduction in ENSO amplitude recorded in coral oxygen isotope ratios. Previous studies have suggested that a change in the ENSO precipitation response over the western Pacific may be due to a northward shift in the ITCZ, leading to a decoupling between atmospheric circulation anomalies and the precipitation response over the region (e.g. Gagan et al. 2004; McGregor and Gagan 2004). In our simulations, there is no evidence of a northward shift in the ITCZ over the western Pacific, and the spatial pattern of western Pacific ENSO–precipitation correlations is not meridionally displaced in any mid-Holocene simulation. However the ability of the model to capture changes in the spatial pattern of ENSO precipitation teleconnections is questionable, as the standard model simulates an incorrect ENSO precipitation response over the western Pacific warm pool. The seasonally flux-adjusted model has a more credible simulation of ENSO teleconnections, but does not capture the reduced mid-Holocene ENSO amplitude. A more detailed discussion of issues in quantitative model–proxy intercomparison will be addressed in future study.

The seasonally flux-adjusted unperturbed and perturbed physics model versions do not simulate a mid-Holocene reduction in ENSO amplitude or systematic change in ENSO frequency. The wide range of ENSO amplitudes displayed by the perturbed physics model versions in pre-industrial simulations is in contrast with the relative insensitivity of ENSO in these model versions to mid-Holocene orbital forcing. It appears that the model ENSO behaviour (at least in a configuration with seasonally-varying flux-adjustment) is more sensitive to internal model physical parameterisations than to climate forcing, confirming that predictions of ENSO sensitivity to climate change remain highly model-dependent.

Several factors contribute to the reduction in ENSO amplitude in the HadCM3 and HadCM3.0A mid-Holocene simulations (and the absence of a change in the HadCM3.0 and perturbed physics simulations). Associated with a stronger Asian summer monsoon circulation, the easterly trade winds are strengthened in the western and central tropical Pacific, from July onwards in HadCM3 runs and August–September onwards in HadCM3.0A runs, persisting until January–February. The stronger trade winds damp positive SST anomalies in the equatorial Pacific and contribute to an earlier termination of El Niño events in these

mid-Holocene simulations. The trade winds also strengthen from boreal autumn onwards in the seasonally flux-adjusted mid-Holocene runs, but the addition of a large positive heat flux in the central Pacific appears to disrupt ocean-atmosphere feedbacks and allow warm SST anomalies to persist in these simulations. A more complete investigation of the interaction between heat flux adjustments and the evolution of El Niño events in HadCM3 is beyond the scope of this study, but it is clear that the use of flux adjustments substantially complicates the interpretation of palaeo-ENSO behaviour.

We can now begin to assess the credibility of predictions of future ENSO change from the versions of HadCM3 examined in this study. The standard version of HadCM3 simulates a reduction in mid-Holocene ENSO amplitude which is in qualitative agreement with the available palaeoclimate proxy evidence, whereas the model versions with seasonally-varying flux adjustments do not reproduce expected ENSO sensitivity to mid-Holocene orbital forcing. By this criterion, the standard version of HadCM3 has a more credible simulation of ENSO sensitivity. However the mean state biases present in the standard model version result in biases in the simulation of ENSO–monsoon interactions and precipitation teleconnections, making comparison with local proxy records problematic. The constant flux-adjusted model version also simulates a reduction in mid-Holocene ENSO amplitude, which is qualitatively consistent with proxy records. However, this model version produces a tropical Pacific climate and ENSO seasonal phase-locking which are not in close agreement with observations, reducing confidence in predictions from this model version.

In the absence of a perfect model, this study supports the use of ensembles of models or perturbed physics model versions in order to explore model ENSO sensitivity to past and future climate forcing. Weighting of coupled model predictions of ENSO based on instrumental data can be supplemented by weighting based on palaeoclimate reconstructions from proxy data. Further work will require a larger ensemble of perturbed physics model versions as well as multi-model ensembles, and a more comprehensive set of palaeo-data against which to validate simulations. In order to use palaeoclimate simulations to weight model predictions, quantitative targets such as mean tropical Pacific SSTs and ENSO amplitude and frequency must be well defined. More robust reconstructions of tropical climate variability will require proxy records from a range of locations and sources, for example including records from the eastern, central and western tropical Pacific. In addition, such studies will need to refine techniques for the quantitative comparison of global climate model output with proxy records which respond to regional climate variability.

References

AchutaRao K, Sperber KR (2002) Simulation of the El Niño southern oscillation: results from the coupled model intercomparison project. Clim Dyn 19:191–209

AchutaRao K, Sperber KR (2006) ENSO simulation in coupled ocean–atmosphere models: are the current models any better? Clim Dyn 27:1–15 DOI 10.1007/s00382-006-0119-7

Berger A (1978) Long-term variations of daily insolation and quaternary climate changes. J Atmos Sci 35:2362–2367

Braconnot P, Joussaume S, Marti O, de Noblet N (1999) Synergistic feedbacks from ocean and vegetation on the African monsoon response to mid-Holocene insolation. Geophys Res Lett 26:2481–2484

Braconnot P, Marti O, Joussaume S, Leclainche Y (2000) Ocean feedback in response to 6 kyr BP insolation. J Clim 13:1537–1553

Brown J, Collins M, Tudhope A (2006) Coupled model simulations of mid-Holocene ENSO and comparisons with coral proxy records. Adv Geosci 6:29–33

Bush A (1999) Assessing the impact of Mid-Holocene insolation on the atmosphere-ocean system. Geophys Res Lett 26:99–102

Cane MA (2005) The evolution of El Niño, past and future. Earth Planet Sci Lett 230:227–240

Chappallaz J, Blunier T, Kints S, Dallenbach A, Barnola J, Schwander J, Raynaud D, Stauffer B (1997) Changes in the atmospheric CH_4 gradient between Greenland and Antarctica during the Holocene. J Geophys Res 15987–15999

Clement AC, Seager R, Cane MA (2000) Suppression of El Niño during the mid-Holocene by changes in the Earth's orbit. Paleoceanography 15:731–737

Clement A, Cane M, Seager R (2001) An orbitally driven tropical source for abrupt climate change. J Clim 14:2369–2375

Collins M (2000) Understanding uncertainties in the response of ENSO to greenhouse warming. Geophys Res Lett 27:3509–3513

Collins M, Tett SFB, Cooper C (2001) The internal climate variability of HadCM3, a version of the Hadley Centre coupled model without flux adjustments. Clim Dyn 17:61–81

Collins M, The CMIP modelling groups (2005) El Niño- or La Niña-like climate change. Clim Dyn 24:89–104

Collins M, Booth BB, Harris GR, Murphy JM, Sexton DMH, Webb MJ (2006) Towards quantifying uncertainty in transient climate change. Clim Dyn 27:127–147 DOI 10.1007/s00382-006-0121-0

Fedorov AV, Philander SG (2000) Is El Niño changing? Science 288:1997–2002

Gagan MK, Ayliffe LK, Hopley D, Cali JA, Mortimer GE, Chappell J, McCulloch MT, Head MJ (1998) Temperature and surface-ocean water balance of the mid-Holocene tropical western Pacific. Science 279:1014–1018

Gagan MK, Hendy EJ, Haberle SG, Hantoro WS (2004) Post-glacial evolution of the Indo-Pacific Warm Pool. Quat Int 118–119:127–143

Ganopolski A, Kubatzki C, Claussen M, Brovkin V, Petoukhov V (1998) The influence of vegetation-atmosphere-ocean interaction on climate during the mid-Holocene. Science 280:1916–1919

Gordon C, Cooper C, Senior CA, Banks H, Gregory JM, Johns TC, Mitchell JFB, Wood RA (2000) The simulation of SST, sea ice

extent and ocean heat transports in a version of the Hadley Centre coupled model without flux adjustments. Clim Dyn 16:147–168

Guilyardi E (2006) El Niño–mean state–seasonal cycle interactions in a multi-model ensemble. Clim Dyn 26:329–348 DOI 10.1007/s00382-005-0084-6

Harrison SP, Jolly D, Laarif F, Abe-Ouchi A, Dong B, Herterich K, Hewitt C, Joussaume S, Kutzbach JE, Mitchell J, de Noblet N, Valdes P (1998) Intercomparison of simulated global vegetation distributions in response to 6 kyr BP orbital forcing. J Clim 11:2721–2742

Haug GH, Hughen KA, Sigman DM, Peterson LC, Rohl U (2001) Southward migration of the Intertropical Convergence Zone through the Holocene. Science 293:1304–1307

Hewitt CD, Mitchell JFB (1998) A fully coupled GCM simulation of the climate of the mid-Holocene. Geophys Res Lett 25:361–364

Indermuhle A, Stocker TF, Joos F, Fischer H, Smith HJ, Wahlen M, Deck B, Mastroianni D, Tschumi J, Blunier T, Meyer R, Stauffer B (1999) Holocene carbon-cycle dynamics based on CO_2 trapped in ice at Taylor Dome, Antarctica. Nature 398:121–126

Inness PM, Slingo JM, Guilyardi E, Cole J. (2003) Simulation of the Madden-Julian Oscillation in a coupled general circulation model. Part II: the role of the basic state. J Clim 16:365–382

Joussaume S, Taylor KE, Braconnot P, Mitchell JFB, Kutzbach JE, Harrison SP, Prentice IC, Broccoli AJ, Abe-Ouchi A, Bartlein PJ, Bonfils C, Dong B, Guiot J, Herterich K, Hewitt CD, Jolly D, Kim JW, Kislov A, Kitoh A, Loutre MF, Masson V, McAvaney B, McFarlane N, de Noblet N, Peltier WR, Peterschmitt JY, Pollard D, Rind D, Royer JF, Schlesinger ME, Syktus J, Thompson S, Valdes P, Vettorett G, Webb RS, Wyputta U (1999) Monsoon changes for 6000 years ago: results of 18 simulations from the Paleoclimate Modeling Intercomparison Project (PMIP). Geophys Res Lett 26(7):859–862

Kitoh A, Murakami S (2002) Tropical Pacific climate at the mid-Holocene and the Last Glacial Maximum simulated by a coupled ocean-atmosphere general circulation model. Paleoceanography 17:1047 DOI 10.1029/2001PA000724

Koutavas A, Lynch-Stieglitz J, Marchitto TM, Sachs JP (2002) El Niño-like pattern in Ice Age tropical Pacific sea surface temperature. Science 297:226–230

Knutti R, Meehl GA, Allen MR, Stainforth DA (2006) Constraining climate sensitivity from the seasonal cycle in surface temperature. J Clim 19:4224–4233

Lea DW, Pak DK, Belanger CL, Spero HJ, Hall MA, Shackleton NJ (2006) Paleoclimate history of Galápagos surface waters over the last 135,000 yr. Quat Sci Rev 25:1152–1167

Latif M, Sperber K, Arblaster J, Braconnot P, Chen D, Colman A, Cubasch U, Cooper C, Delecluse P, DeWitt D, Fairhead L, Flato G, Hogan T, Ji M, Kimoto M, Kitoh A, Knutson T, Le Treut H, Li T, Manabe S, Marti O, Mechoso C, Meehl G, Power S, Roeckner E, Sirven J, Terray L, Vintzileos A, Voss R, Wang B, Washington W, Yoshikawa I, Yu J, Zebiak S (2001) ENSIP: the El Niño simulation intercomparison project. Clim Dyn 18:255–276

Liu Z, Kutzbach J, Wu L (2000) Modeling climate shift of El Niño variability in the Holocene. Geophys Res Lett 27:2265–2268

Liu Z, Otto-Bliesner B, Kutzbach J, Li L, Shields C (2003) Coupled model simulation of the evolution of global monsoons in the Holocene. J Clim 16:2472–2490

Liu Z, Harrison SP, Kutzbach J, Otto-Bliesner B (2004) Global monsoons in the mid-Holocene and oceanic feedback. Clim Dyn 22:157–182

McGregor HV, Gagan MK (2004) Western Pacific coral $\delta^{18}O$ records of anomalous Holocene variability in the El Niño-Southern Oscillation. Geophys Res Lett L11204 DOI 10.1029/2004GL019972

Meehl GA, Gent PR, Arblaster JM, Otto-Bliesner BL, Brady EC, Craig A (2001) Factors that affect the amplitude of El Niño in global coupled climate models. Clim Dyn 17:515–526

Merryfield WJ (2006) Changes to ENSO under CO_2 doubling in a multi-model ensemble. J Clim 19:4009:4027

Moy CM, Seltzer GO, Rodbell DT, Anderson DM (2002) Variability of El Niño/Southern Oscillation activity at millennial timescales during the Holocene epoch. Nature 420:162–165

Murphy J, Sexton D, Barnett D, Jones G, Webb M, Collins M, Stainforth D (2004) Quantification of modelling uncertainties in a large ensemble of climate change simulations. Nature 430:768–772

Otto-Bliesner B, Brady E, Shin S, Liu Z, Shields C (2003) Modeling El Niño and its tropical teleconnections during the last glacial-interglacial cycle. Geophys Res Lett 30 DOI 10.1029/2003GL018553

Piani C, Frame DJ, Stainforth DA, Allen MR (2005) Constraints on climate change from a multi-thousand member ensemble of simulations. Geophys Res Lett 32:L23825 DOI 10.1029/2005GL024452

Pope VD, Gallani ML, Rowntree PR, Stratton RA (2000) The impact of new physical parametrizations in the Hadley Centre climate model–HadAM3. Clim Dyn 16:123–146

Rayner NA, Parker DE, Horton EB, Folland CK, Alexander LV, Rowell DP, Kent EC, Kaplan A (2003) Global analyses of sea surface temperature, sea ice, and night marine air temperature since the late nineteenth century. J Geophys Res 108:4407 DOI 10.1029/2002JD002670

Rodbell DT, Seltzer GO, Anderson DM, Abbott MB, Enfield DB, Newman JH (1999) An ~15,000 year record of El Niño-driven alluviation in southwestern Ecuador. Science 283:516–520

Sandwiss DH, Richardson JB, Reitz EJ, Rollins HB, Maasch KA (1996) Geoarchaeological evidence from Peru for a 5000 year B.P. onset of El Niño. Science 273:1531–1533

Spencer H, Sutton R, Slingo JM (2007) El Niño in a coupled climate model: sensitivity to changes in mean state induced by heat flux and wind stress corrections. J Clim (in press)

Stott L, Cannariato K, Thunell R, Haug GH, Koutavas A, Lund S (2004): Decline of surface temperature and salinity in the western tropical Pacific Ocean in the Holocene epoch. Nature 431:56–59

Tebaldi C, Smith RL, Nychka D, Mearns LO (2005) Quantifying uncertainty in projections of regional climate change: A Bayesian approach to the analysis of multi-model ensembles. J Clim 18:1524–1540

Toniazzo T (2006) A study of the sensitivity of ENSO to the mean climate. Adv Geosci 6:111–118

Toniazzo T, Collins M, Brown J (2007) The variation of ENSO characteristics associated with atmospheric parameter perturbations in a coupled model. Clim Dyn (submitted)

Tudhope AW, Chilcott CP, McCulloch MT, Cook ER, Chappell J, Ellam RM, Lea DW, Lough JM, Shimmield GB (2001) Variability in the El Niño-Southern Oscillation through a glacial-interglacial cycle. Science 291:1511–1517

Turner AG, Inness PM, Slingo JM (2005) The role of the basic state in the ENSO-monsoon relationship and implications for predictability. Quart J R Meteorol Soc 131:781–804

Tziperman E, Zebiak SE, Cane MA (1997) Mechanisms of seasonal–ENSO interaction. J Atmos Sci 54:61–71

van Oldenborgh GJ, Philip S, Collins M (2005) El Niño in a changing climate: a multi-model study. Ocean Sci Discuss 2:267–298

Wang C, Picaut J (2004) Understanding ENSO physics: a review. In: Wang C, Xie S-P, Carton JA (eds) Earth's climate: the ocean-atmosphere interaction, geophysical monograph series, AGU, Washington, pp 21–48

Webb MJ, Senior CA, Sexton DMH, Ingram WJ, Williams KD, Ringer MA, McAvaney BJ, Colman R, Soden BJ, Gudgel R, Knutson T, Emori S, Ogura T, Tsushima Y, Andronova N, Li B, Musat I, Bony S, Taylor KE (2006) On the contribution of local feedback mechanisms to the range of climate sensitivity in two GCM ensembles. Clim Dyn 27:17–38

Webster P, Yang S (1992) Monsoon and ENSO: selectively interacting systems. Quart J R Meterol Soc 118:877–926

Zebiak SE, Cane MA (1987) A model El Niño/Southern Oscillation. Month Weather Rev 115:2262–2278

Zhao Y, Braconnot P, Marti O, Harrison SP, Hewitt C, Kitoh A, Liu Z, Mikolajewicz U, Otto-Bliesner B, Weber SL (2005) A multi-model analysis of the role of the ocean on the African and Indian monsoon during the mid-Holocene. Clim Dyn 25:777–800